Surface & Coatings Technology 357 (2019) 379–383

Contents lists available at ScienceDirect

Surface & Coatings Technology

journal homepage: www.elsevier.com/locate/surfcoat

Abrasion and erosion behavior of DLC-coated oil-well tubings in a heavy oil/sand environment☆

Liangliang Liu[a], Zhongzhen Wu[a,b,d,*], Suihan Cui[a], Xiaokai An[a], Zhengyong Ma[a], Tielei Shao[a], Ricky K.Y. Fu[b], Ruijun Wang[c], Hai Lin[a], Feng Pan[a], Paul K. Chu[b,d,**]

[a] School of Advanced Materials, Peking University Shenzhen Graduate School, Shenzhen 518055, China
[b] Department of Physics, City University of Hong Kong, Tat Chee Avenue, Kowloon, Hong Kong, China
[c] Surface Engineering and Technology Institute,Chinese Academy of Agricultural Machanization Science, Beijing 100083, China
[d] Department of Materials Science and Engineering, City University of Hong Kong, Tat Chee Avenue, Kowloon, Hong Kong, China

ARTICLE INFO

Keywords:
Abrasion and corrosion
DLC coatings
Thickness
Heavy oil sand environment

ABSTRACT

The sucker rod pump, an important machine in oil exploration and extraction, normally works in a heavy oil and sand environment in which severe abrasion and erosion occur, especially on oil-well tubings. To improve the service life, DLC coatings with different thicknesses are fabricated on the oil-well tubings and the mechanical, tribological, and anti-corrosion properties are investigated. The results show that the thickness can be compromised with adhesion due to the low stress induced by alternate implantation and deposition at the pulsed high-voltage bias. Compared to severe abrasion of the carbonitriding AISI 1045 oil-well tubing, the thick DLC coatings have good anti-abrasion properties in the heavy oil and sand environment. Moreover, excellent erosion resistance is observed from the DLC-coated samples as exemplified by the small corrosion current density and high corrosion potential. The tests conducted in both simulated and practical working conditions reveal that the service life of the oil-well tubing is significantly improved.

1. Introduction

The sucker rod pump, an important machine in oil exploration and extraction, usually works in the heavy oil and sand environment in which severe abrasion and erosion occur, especially for oil-well tubings due to the low hardness, poor tribological and corrosion resistance of structural materials such as AISI (American Iron and Steel Institute) 1020 and AISI 1045 [1–3]. Usually, carbonitriding and application of Ni and Ti based hard coatings are used to improve the surface strength of the components [6–9]. However, there are some drawbacks such as large friction coefficients of Ti-based coatings, low erosion resistance of Fe-based surface, and so on [10].

Diamond-like carbon (DLC) coatings possessing high hardness, low friction coefficient, and excellent corrosion resistance have been demonstrated to be suitable for applications in the heavy oil and sand environment [11–13]. However, owing to the high internal stress of the DLC coatings and in order to avoid delamination, the thickness is limited to 1–3 μm [11]. Small friction coefficients are usually obtained by hydrogen doping of DLC coatings with H containing gases such as CH_4 or C_2H_2, but the coating hardness may be compromised leading to more severe abrasion. In fact, neither a small thickness nor low hardness can provide sufficient protection in the heavy oil and sand environment. Therefore, thick DLC coatings with excellent adhesion and hardness are indispensable [14,15]. In our previous works [16], the internal stress of DLC coatings could be reduced by alternating implantation and deposition induced by a pulsed kV bias together with the fabrication of an optimized Cr/CrCx/CrC interlayer and ion-based interfacial treatment [17]. High adhesion (> 70 N) and large coating thickness (> 50 μm) are achieved for the hard (about 20 GPa) DLC coatings rendering them potentially useful in the harsh environments.

In this work, DLC coatings are fabricated on oil-well tubings and the effects of the coating thickness on the abrasion and erosion characteristics in the heavy oil and sand environment are evaluated. Thick DLC coatings (> 9 μm) exhibit both higher adhesion and more attractive abrasion and erosion resistance in this environment due to lower internal stress and high bearing capacity. The coated oil-well tubing has significantly increased serve life (5 times) according to the results obtained under simulated and practical working conditions.

☆ The 14th International Conference on Plasma Based Ion Implantation & Deposition(PBII&D 2017) ID: 96.

* Correspondence to: Z.Z. Wu, School of Advanced Materials, Peking University Shenzhen Graduate School, Shenzhen 518055, China.
** Correspondence to: P.K. Chu, Department of Physics, City University of Hong Kong, Tat Chee Avenue, Kowloon, Hong Kong, China.
E-mail addresses: wuzz@pkusz.edu.cn (Z. Wu), paul.chu@cityu.edu.hk (P.K. Chu).

https://doi.org/10.1016/j.surfcoat.2018.09.081
Received 28 March 2018; Received in revised form 30 June 2018; Accepted 4 September 2018
Available online 01 October 2018

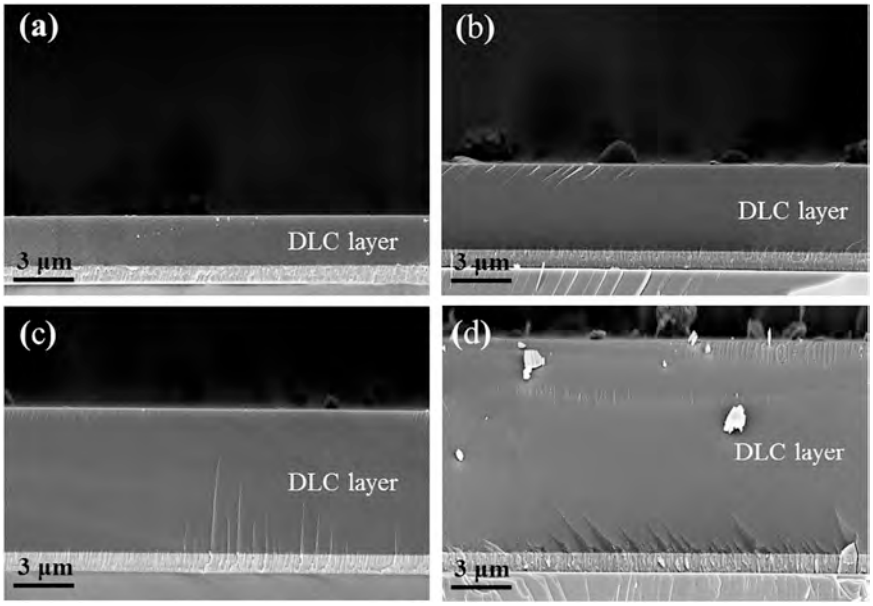

Fig. 1. SEM cross-sectional images of samples deposited for different time: (a) 3 h, (b) 6 h, (c) 9 h, (d) 12 h.

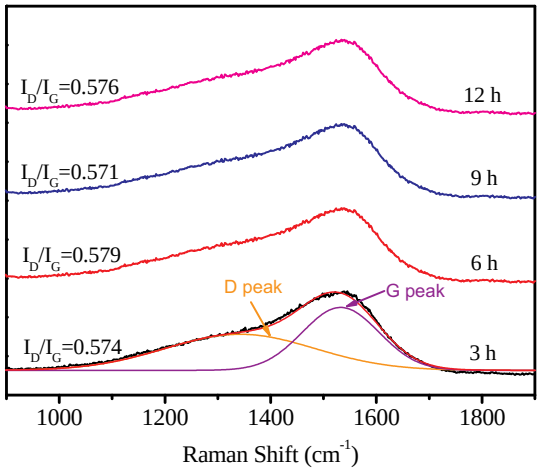

Fig. 2. Raman scattering spectra of DLC coatings with different thicknesses.

2. Experimental details

Polished P-type Si (100) wafers (20 × 10 × 0.5 mm) and carbonitriding AISI 1045 steel pieces (20 × 30 × 1 mm) were used as substrates. The AISI 1045 substrates were manually ground using abrasive SiC paper from 320 grits to 1500 grits and polished with 1 μm diamond paste using a velvet cloth. The samples were ultrasonically cleaned in acetone, alcohol, and deionized water to remove polishing residues. They were stored in an oven at 100 °C before deposition which was carried out in a vacuum chamber 100 cm in diameter and 80 cm in height. The temperature in the chamber was increased gradually to 200 °C and the vacuum system was evacuated to a base pressure of 3×10^{-3} Pa. Before deposition, the substrate was cleaned with Ar ions at a pressure of 0.8 Pa and bias voltage of −600 V for 20 min. The optimized Cr/CrCx/CrC interlayer was fabricated by high-power impulse magnetron sputtering (HiPIMS) in Ar (99.999% pure) and C_2H_2 (99.8% pure) using a Cr target. The DLC coatings were deposited at a pulsed bias (−7500 V, 50 Hz, 100 μs) using an anode layer ion source in a gas mixture of 10 sccm Ar and 45 sccm C_2H_2, and the sample holder

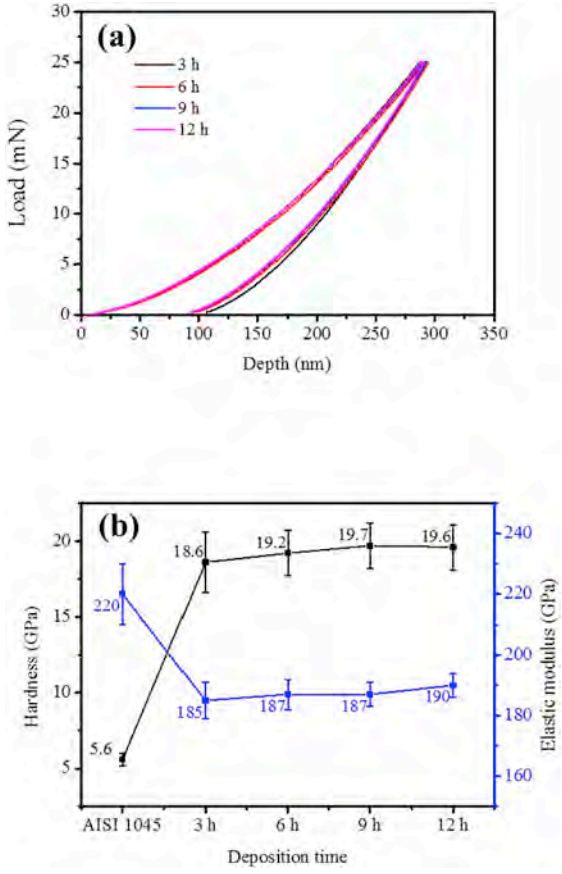

Fig. 3. Nanoindentation results: (a) Load versus displacement curves and (b) Hardness and elastic moduli of different samples.

was fixed at 15 cm in front of the ion source during deposition. In order to study the effects of the DLC thickness on abrasion, coatings were deposited for 3 h, 6 h, 9 h, and 12 h.

Field-emission scanning electron microscopy (FE-SEM, ZEISS

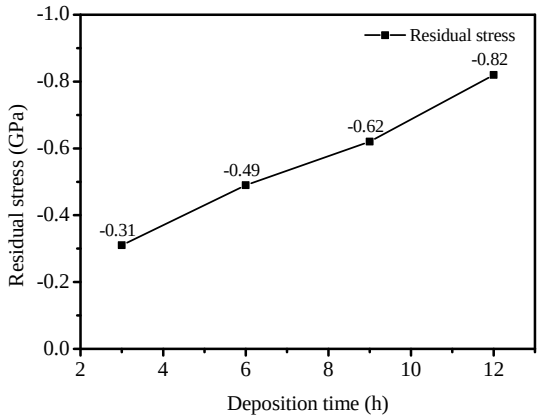

Fig. 4. Residual stresses of the DLC coatings with different thicknesses.

SUPRA® 55) was used to examine the morphology and measure the coating thickness. The structure of the DLC coatings was determined on a Raman spectro-meter (Horiba LAabRam HR VIS) with a 532 nm laser as the excitation source. In order to exclude the substrate effect, nanoindentation (Ti - 750,Hystrion, America) was used to determine the microhardness at a maximum load of 25 mN. The residual stress was measured by a film stress tester (FST100, SuPro Instruments, China), which is calculated by Stoney equation based on substrate curvature method. A scratch test instrument (WS - 2005, Zhongke Kaihua Technology, China) was employed to determine the adhesion strength between the coatings and substrate. A progressive load from 0 N to 100 N was applied at 3 mm/min and 50 N/min. A multifunction tribometer (MFT - 5000, Rtec Instruments, America) was used to determine the friction coefficients and abrasion characteristics of the DLC coated samples against 5 × 5 × 2 mm AISI 1045 steel in the heavy oil and sand environment at a load of 10 N and wear length of 10 mm. In order to simulate the practical working conditions of the oil-well tubings, the tribometer was refitted with the part of the tubes and the heavy oil and sand came from the oil field. The corrosion resistance was measured on an electrochemical workstation (CHI-604E, Shanghai Shenhua, China).

3. Results and discussion

Fig. 1 shows the cross-sectional SEM images of the Cr/CrCx/CrC/DLC coatings deposited on Si substrates for different deposition time. The Cr/CrCx/CrC interlayers and DLC layer can be identified clearly. The Cr/CrCx/CrC interlayer with an optimal thickness of 0.8–1.0 μm releases the internal stress and forms strong adhesion between the substrate and DLC coatings [16]. The thicknesses of the DLC layers are about 2.7 μm, 5.3 μm, 8.3 μm, and 11 μm, respectively, depending on the deposition time. A typical amorphous carbon structure exists in the DLC layers and there is no obvious difference except thickness among the samples deposited using similar parameters.

Fig. 2 presents the Raman scattering spectra of the four DLC coated samples for different deposition time. As a common technique to characterize DLC [18], the typical Raman scattering spectra exhibit an asymmetrical peak in 1000–1800 cm^{-1} corresponding to the characteristic D and G bands for the DLC phase [19,20] and the intensity, peak position, and full-width at half-maximum (FWHM) of the D and G bands can be used to characterize the properties of DLC coatings. In particular, the intensity ratio of the D and G peaks (I_D/I_G) is correlated to the sp^3/sp^2 bonding ratio. A smaller I_D/I_G ratio indicates a larger percentage of sp^3 hybridized carbon [21,22]. The D and G peaks are deconvoluted by Gaussian fitting. A small I_D/I_G ratio of 0.57 is observed and the variation is small with different thicknesses, indicating stable deposition independent of deposition time.

Fig. 3(a) shows the load vs. displacement curves at a maximum load of 25 mN obtained by nanoindentation. All the samples show a similar maximum penetration depth of about 290 nm. The residual penetration depth of the 3 h sample is about 110 nm and that of the other three samples is about 90 nm. The difference may be attributed to the thickness (about 2.7 μm with the deposition time of 3 h) which is too thin to avoid contributions from the substrate (penetration depth exceeding 10% of the DLC thickness) [23–25]. The hardness (H) and elastic modulus (E) are calculated according to the load vs. displacement curves as presented in Fig. 3(b). With the exception of the thinnest sample, the DLC coatings show similar hardnesses of about 19.2 GPa,

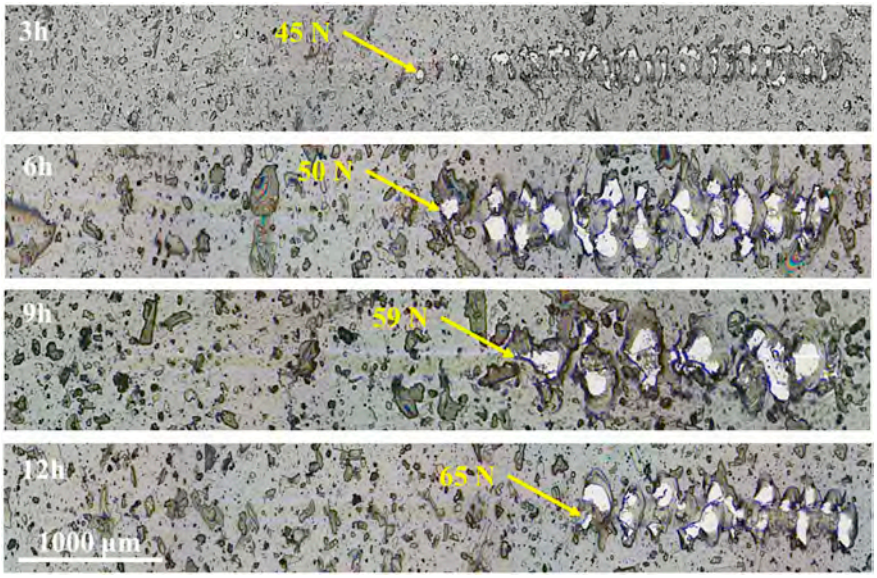

Fig. 5. Scratch test results of the DLC coatings with different thicknesses.

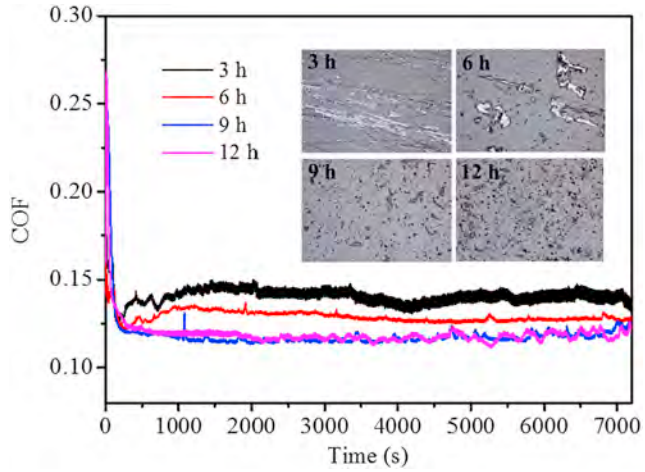

Fig. 6. Friction coefficients and surface morphology of abrasion tracks on the DLC coatings with different thicknesses.

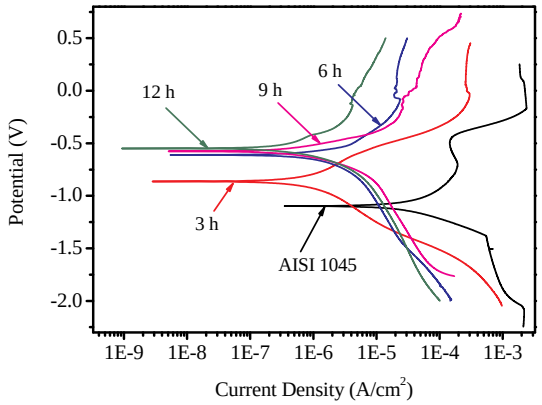

Fig. 7. Potentiodynamic tests of the AISI 1045 substrate and different samples.

Table 1
I_{corr} and E_{corr} of yjr AISI 1045 substrate and different samples.

Sample	E_{corr}/mV	I_{corr}/μA·cm^{-2}
AISI 1045	−1095.7	44.73
3 h	−859.1	1.14
6 h	−607.8	1.76
9 h	−683.6	1.31
12 h	−545.1	1.98

19.7 GPa and 19.6 GPa, respectively, which is about three times that of the substrate. The elastic moduli are consistent with the hardness.

The residual stress of DLC coatings with different thickness are measured and shown in Fig. 4. With the increasing thickness, the residual stresses for the four samples are −0.31 GPa, −0.49 GPa, −0.62 GPa and −0.82 GPa, respectively. Scratch tests are performed to detect the adhesions of the coatings on the substrate, which is the most common failure mode of thick DLC coatings. Fig. 5 shows the optical images of the scratch tracks of the samples with different thickness. Interestingly, although the same interlayer and deposition parameters, the adhesion of the different samples present significant difference. The critical load of the thinnest sample is 45 N, and it increases to 65 N gradually with increasing the DLC thickness. This unusual phenomenon indicates that stress accumulation is not the determinant of the adhesion because of the small absolute value produced by the alternate implantation and deposition with pulsed high-voltage bias [17], but the thickness which can provide higher load-bearing capacity than thinner DLC coatings becomes the determinant of the adhesion [14,15].

The friction coefficients of the DLC coatings against AISI 1045 steel in the heavy oil and sand environment are presented in Fig. 6(a). A larger friction coefficient of about 0.14 and a broader curve are observed from the thinnest DLC coating. With increasing DLC thickness, the friction coefficients decrease gradually and the curve becomes narrower. Owing to the large amount of sand in the oil, abrasion is exacerbated thus producing fluctuations in the friction coefficient curve. They are especially obvious for thin coatings. The surface morphology of the tracks is displayed in Fig. 6. As expected, the surface of the thinnest sample is full of scratches caused by sand and most of the scratches are deep up to the substrate, thus indicating failure of DLC coating and fluctuating friction coefficients. The exfoliation areas observed on the surface are supposed as the synergistic effect of wear and corrosion [26,27]. With increase coating thickness, only some tiny scratches can be observed implying improved abrasion resistance performance in the heavy oil and sand environment. The excellent abrasion resistance of the thicker DLC coatings results from the higher load-bearing capacity against hard sand particles.

The electrochemical corrosion behavior is investigated by potentiodynamic tests. The polarization curves and details of I_{corr} and E_{corr} of the different samples and those of the substrate are presented in Fig. 7 and Table. 1, respectively. The AISI 1045 substrate has a low E_{corr} of −1095.7 mV and large I_{corr} of 44.73 μA·cm^{-2} indicative of poor corrosion resistance. All the coated samples show bigger E_{corr} and smaller I_{corr}. With increasing DLC thickness, the corrosion resistance increases and the thickest one have the best corrosion resistance.

In order to simulate the practical working conditions of oil-well tubings, the tribometer is refitted with the cutted tubes as shown in Fig. 8(a1) (Video 1 in supporting files). The external surface of the inner oil-well tubing is coated with 12 μm thick DLC, whereas the inner side of the out oil-well tubing is carbonitrided for comparison. Many deep scratches can be observed in Fig. 8(a2) from the surface of the failed oil-well tubing after actual use for three months. Similar scratches are observed from the carbonitrided oil-well tubing after 15,000 test cycles on the test machine but no obvious scratches appear from the DLC coated sample. Further tests show deep scratches up to the substrate after 75,000 test cycles on the DLC coated oil-well tubing. The significantly improved service life can also be observed after the practical working test as shown in Fig. 8 (b1–b5). Compared to the 3 month's working life of the carbonitrided oil-well tubing, the DLC coated sample starts to fail after 15 months for an improvement of 5 times over the uncoated one.

4. Conclusion

To improve the service life of the oil-well tubing, DLC coatings with different thicknesses are fabricated on AISI 1045 steel. The morphology, structure, mechanical properties, abrasion resistance, and corrosion resistance are investigated. The DLC coatings with different thicknesses do not show significant differences in the structure and mechanical properties while adhesion increases gradually from 45 N to 65 N due to the lower internal stress and higher bearing capacity for thicker DLC coatings. Consequently, the thicker DLC coatings have better abrasion and erosion resistance in the heavy oil and sand environment. Tests conducted under the simulated and practical working conditions reveal that the service life of the oil-well tubings is improved by 5 times.

Supplementary data to this article can be found online at https://doi.org/10.1016/j.surfcoat.2018.09.081.

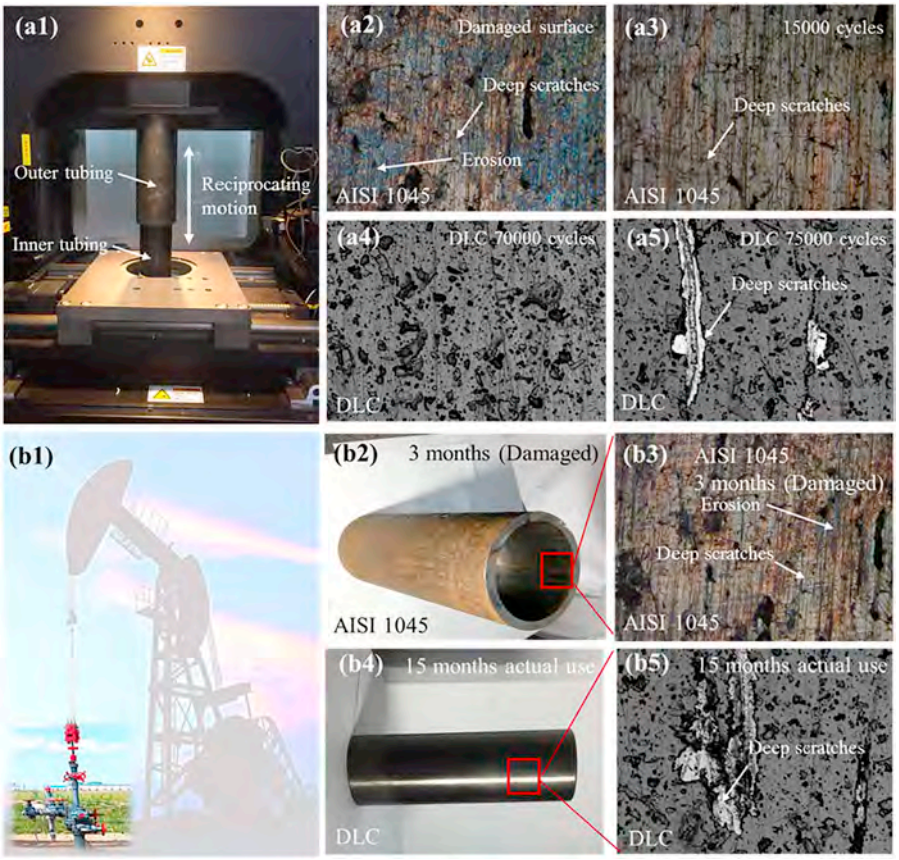

Fig. 8. Results of oil-well tubings on the test machine: (a1–a5) Simulated conditions; (b1–b5) Actual use.

Acknowledgements

This work was financially supported by National Materials Genome Project (No. 2016YFB0700600), Shenzhen Science and Technology Innovation Commission Research Grants (JCYJ20150828093127698), and City University of Hong Kong Applied Research Grant (ARG) No. 9667122.

References

[1] I. Akhyar, M. Sayuti, Effect of heat treatment on hardness and microstructures of AISI 1045, Adv. Mater. Res. 1119 (2015) 575–579.
[2] Q.H. Li, T.M. Yue, Z.N. Guo, et al., Microstructure and corrosion properties of AlCoCrFeNi high entropy alloy coatings deposited on AISI 1045 steel by the electrospark process, Metall. Mater. Trans. A 44 (4) (2013) 1767–1778.
[3] H.D. Wang, D.M. Zhuang, K.L. Wang, et al., Comparative investigation on tribological properties of ion-sulfuration layers under dry friction, Tribol. Lett. 13 (1) (2002) 55–61.
[6] X. Ye, J. Wu, Y. Zhu, et al., A study of the effect of propane addition on plasma nitrocarburizing for AISI 1045 steel, Vacuum 110 (110) (2014) 74–77.
[7] H. Liu, J. Li, Y. Chai, et al., A novel plasma oxynitriding by using plain air for AISI 1045 steel, Vacuum 121 (2015) 18–21.
[8] C. Zhao, F. Tian, H.R. Peng, et al., Non-transferred arc plasma cladding of Stellite Ni60 alloy on steel, Surf. Coat. Technol. 155 (1) (2002) 80–84.
[9] H. Liu, C. Wang, X. Zhang, et al., Improving the corrosion resistance and mechanical property of 45 steel surface by laser cladding with Ni60CuMoW alloy powder, Surf. Coat. Technol. 228 (8) (2013) S296–S300.
[10] J. Hardell, B. Prakash, Tribological performance of surface engineered tool steel at elevated temperatures, Int. J. Refract. Met. Hard Mater. 28 (1) (2010) 106–114.
[11] A. Grill, Diamond-like carbon: state of the art, Diam. Relat. Mater. 8 (2–5) (1999) 428–434.
[12] M. Tabbal, P. Merel, M. Chaker, et al., Effect of laser intensity on the microstructural and mechanical properties of pulsed laser deposited diamond-like-carbon thin films, J. Appl. Phys. 85 (7) (1999) 3860–3865.
[13] A.H. Jayatissa, F. Sato, N. Saito, et al., Characterization of diamond-like carbon clusters deposited by pulsed ArF laser deposition, Carbon 38 (8) (2000) 1145–1151.
[14] J. Wang, J. Pu, G. Zhang, et al., Architecture of superthick diamond-like carbon films with excellent high temperature wear resistance, Tribol. Int. 81 (2015) 129–138.
[15] J. Wang, J. Pu, G. Zhang, et al., Interface architecture for Superthick carbon-based films toward low internal stress and ultrahigh load-bearing capacity, ACS Appl. Mater. Interfaces 5 (11) (2013) 5015–5024.
[16] L. Liu, Z. Wu, X. An, et al., Excellent adhered thick diamond-like carbon coatings by optimizing hetero-interfaces with sequential highly energetic Cr and C ion treatment, J. Alloys Compd. 735 (2018) 155–162.
[17] X.K. An, Z.Z. Wu, L.L. Liu, et al., High-ion-energy and low-temperature deposition of diamond-like carbon (DLC) coatings with pulsed kV bias, Surf. Coat. Technol. (2018), https://doi.org/10.1016/j.surfcoat.2018.08.099 (Accepted).
[18] W.G. Cui, Q.B. Lai, L. Zhang, et al., Quantitative measurements of sp 3, content in DLC films with Raman spectroscopy, Surf. Coat. Technol. 205 (7) (2010) 1995–1999.
[19] A.C. Ferrari, J. Robertson, Interpretation of Raman spectra of disordered and amorphous carbon, Phys. Rev. B Condens. Matter 61 (20) (2000) 14095–14107.
[20] P.K. Chu, L. Li, Characterization of amorphous and nanocrystalline carbon films, Mater. Chem. Phys. 96 (2–3) (2006) 253–277.
[21] E. Enríquez, M.A.D.L. Rubia, A.D. Campo, et al., Characterization of carbon nanoparticles in thin-film nanocomposites by confocal Raman microscopy, J. Phys. Chem. C 1181 (19) (2014) 10488–10494.
[22] A.C. Ferrari, J. Robertson, Resonant Raman spectroscopy of disordered, amorphous, and diamondlike carbon, Phys. Rev. B Condens. Matter 64 (7) (2001) 075414.
[23] Kumar S. Ishpal, N. Dwivedi, et al., Investigation of radio frequency plasma for the growth of diamond like carbon films, Phys. Plasmas 19 (3) (2012) 033515.
[24] D. Liu, G. Benstetter, E. Lodermeier, et al., Influence of the incident angle of energetic carbon ions on the properties of tetrahedral amorphous carbon (taC) films, J. Vac. Sci. Technol. A 21 (5) (2003) 1665–1670.
[25] H. Liu, Q. Xu, C. Wang, et al., Investigating the microstructure and mechanical behaviors of DLC films on AISI52100 bearing steel surface fabricated by plasma immersion ion implantation and deposition, Surf. Coat. Technol. 228 (2013) S159–S163.
[26] L. Li, L.L. Liu, X. Li, et al., Enhanced tribocorrosion performance of Cr/GLC multilayered films for marine protective application, ACS Appl. Mater. Interfaces 10 (2018) 13187–13198.
[27] L. Peña-Parás, D. Maldonado-Cortés, P. García, et al., Tribological performance of halloysite clay nanotubes as green lubricant additives, Wear s376–377 (2017) 885–892.